

# Geometry of meandering and braided gravel-bed threads from the Bayanbulak Grassland, Tianshan, P.R. China.

F. Métivier<sup>1</sup>, O. Devauchelle<sup>1</sup>, H. Chauvet<sup>1</sup>, E. Lajeunesse<sup>1</sup>, P. Meunier<sup>2</sup>, K. Blanckaert<sup>3</sup>, P. Ashmore<sup>4</sup>, Z. Zhang<sup>5</sup>, Y. Fan<sup>6</sup>, Y. Liu<sup>7</sup>, Z. Dong<sup>5</sup>, and B. Ye<sup>5</sup>

<sup>1</sup>Institut de physique du globe de Paris – Sorbonne Paris Cité, Université Paris Diderot, CNRS, UMR7154, 1 rue Jussieu, 75238 Paris Cedex 05, France

<sup>2</sup>Département de Géologie, UMR8538, CNRS, Ecole Normale Supérieure, 24 rue Lhomond, 75005 Paris, France

<sup>3</sup>Research center for Eco-environmental sciences, Chinese Academy of sciences, Beijing, P.R. China

<sup>4</sup>Department of Geography, Social Science Centre Rm 2322, Western University, London, Ontario, Canada

<sup>5</sup>The States Key laboratory of Cryospheric Science, Cold and Arid Region Environmental and Engineering and Research Institute, Chinese Academy of Sciences 260 Donggang west road, Lanzhou, China

<sup>6</sup>Xinjiang Institute of Ecology and geography, Chinese Academy of Sciences, urumqi, P.R.China

<sup>7</sup>Key Laboratory of Water Environment and Resource, Tianjin Normal University, 393 Binshui west road, Tianjin 300387, China

*Correspondence to:* F. Métivier (metivier@ipgp.fr)

## Abstract

The Bayanbulak Grassland, Tianshan, P.R. China is located in an intramontane sedimentary basin where meandering and braided gravel-bed rivers coexist under the same climatic and geological settings. We report and compare measurements of the discharge, width, depth, slope and grain size of individual threads from these braided and meandering rivers. Both types of threads share statistically indistinguishable regime relations. Their depths and slopes compare well with the threshold theory, but they are wider than predicted by this theory. These findings are reminiscent of previous observations from similar gravel-bed rivers. Using the scaling laws of the threshold theory, we detrend our data with respect to discharge to produce a homogeneous statistical ensemble of width, depth and slope measurements. The statistical distributions of these dimensionless quantities are similar for braided and meandering threads. This suggests that a braided river is a collection of intertwined threads, which individually resemble those of meandering rivers. Given the environmental conditions in Bayanbulak, we furthermore hypothesize that bedload transport causes the threads to be wider than predicted by the threshold theory.

## 1 Introduction

The morphology of alluvial rivers extends between two end-members: in meandering rivers, the flow of water and sediments is confined in a single thread, whereas in braided rivers the flow is distributed into intertwined threads separated by bars (Figure 1; Leopold and Wolman, 1957; Ferguson, 1987; Ashmore, 1991; Schumm, 2005; Kleinhaus and van den Berg, 2011)

Linear stability analyses, supported by laboratory experiments, explain how bedload transport generates bars, and favors the formation of meandering or braided patterns. (Parker, 1976; Fredsøe, 1978; Fujita and Muramoto, 1985; Devauchelle et al., 2007; Ashmore, 1991; Zolezzi et al., 2012). This mechanism proves more efficient in wide and shallow channels. Field measurements indicate that the bankfull aspect ratio (ratio of width to depth) of braided rivers is usually much larger than that of meandering ones, thus suggesting that the bar instability is indeed responsible for braiding (Parker, 1976; Fredsøe, 1978; Fujita and Muramoto, 1985; Devauchelle et al., 2007; Ashmore, 1991; Zolezzi et al., 2012). What exactly controls the aspect ratio of an alluvial river remains an open question, although sediment discharge and riparian vegetation seem significant in this respect: high sediment load and weak vegetation both favour

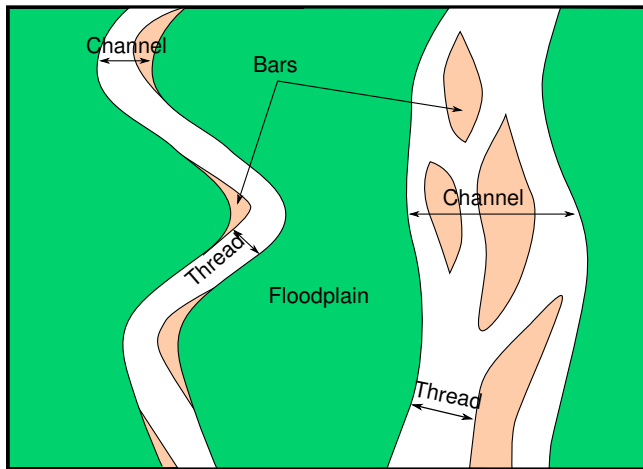


**Figure 1.** Definitions involved in the morphology of meandering (left) and braided (right) rivers (Métivier and Barrier, 2012).

wider and shallower channels, and often induce braiding (Smith and Smith, 1984; Gran and Paola, 2001; Tal and Paola, 2007; Brauderick et al., 2009; Tal and Paola, 2010; Dijk et al., 2012; Métivier and Barrier, 2012).

In a fully-developed braided channel, emerged bars separate the threads from each other (Figure 1), and the very definition of bankfull conditions becomes ambiguous. Most authors treat the channel as a whole by defining lumped quantities, such as the total channel width or the average water depth (Métivier and Barrier, 2012). Conversely, few studies focus on the morphology of braided and meandering channels at the level of individual threads (Church and Gilbert, 1975; Mosley, 1983; Ashmore, 2013; Gaurav et al., 2015). In sand-bed rivers, the geometry of braided threads appears to be indistinguishable from that of meandering ones. This observation accords with recent laboratory experiments (Seizilles et al., 2013; Reitz et al., 2014). To our knowledge, this similarity has not been fully investigated in gravel-bed rivers.

Here, we report on measurements in the Bayanbulak Grassland, Tianshan Mountains, P.R. China, where tens of meandering and braided gravel-bed rivers develop in the same environment. After comparison with other datasets from the literature, we compare the morphology of braided and meandering threads in our dataset. Finally, we rescale our measurements based on the threshold theory to generate and analyse a single statistical ensemble from rivers highly dispersed in size (Glover and Florey, 1951; Henderson, 1963; Seizilles et al., 2013; Gaurav et al., 2015).

## 2 Field site

The Bayanbulak Grassland is an intramontane sedimentary basin standing at an elevation of about 2500 m in the Tianshan Mountains (Figure 2). Two main wetlands, the

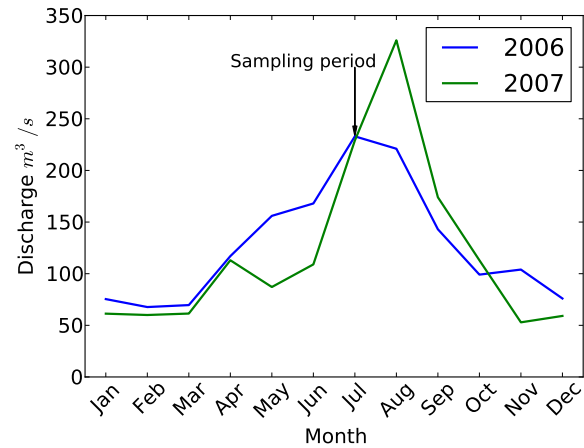


**Figure 3.** Water discharge of the Kaidu River at the Dashankou station, downstream of the grassland (monthly average). Source : Xinjiang Institute for Ecology and Geography.

Qong Yulduz basin (known as the Swan Lake in Chinese), and the Kizik Yulduz basin, are distributed around the main Kaidu River. They are immediately surrounded by sloping meadows (slope  $S \sim 0.01$ ), themselves enclosed with the Tianshan Mountains which provide water to the Kaidu River (Zhang et al., 2002). The hydrology of the basins is controlled by snowmelt and summer orographic precipitations (Zhang et al., 2002; Yang and Cui, 2005). Snow accumulates from November to March, and starts melting in April, inducing the water discharge to rise in all rivers (Zhang et al., 2007). Orographic precipitation takes over in summer (between 260 and 290 mm), and the discharge continues to rise until August (Figure 3).

The morphology of the Bayanbulak rivers varies between highly meandering (sinuosity above 1.3 to 1.5), and braided, and the same river often switches from one to the other along its course (Figures 4 and 5). The rivers span about four orders of magnitude in discharge, and about two in width (Figure 6). Although a variety of grass species grow in the basin, their influence on the channel morphology is probably moderate (Zhang et al., 2002; Andrews, 1984; Métivier and Barrier, 2012). Finally, most rivers flow over gravel, which size distribution does not vary significantly over the basin (Figure 6). All these features combine to make the Bayanbulak Grassland an ideal field site to investigate the morphology of gravel-bed rivers.

## 3 Method

We carried out two field campaigns in July 2012 and July 2013, during the high-flow season to compare the geometry of braided and meandering threads (Figure 3). We treated the threads of braided rivers individually, based on the wetted



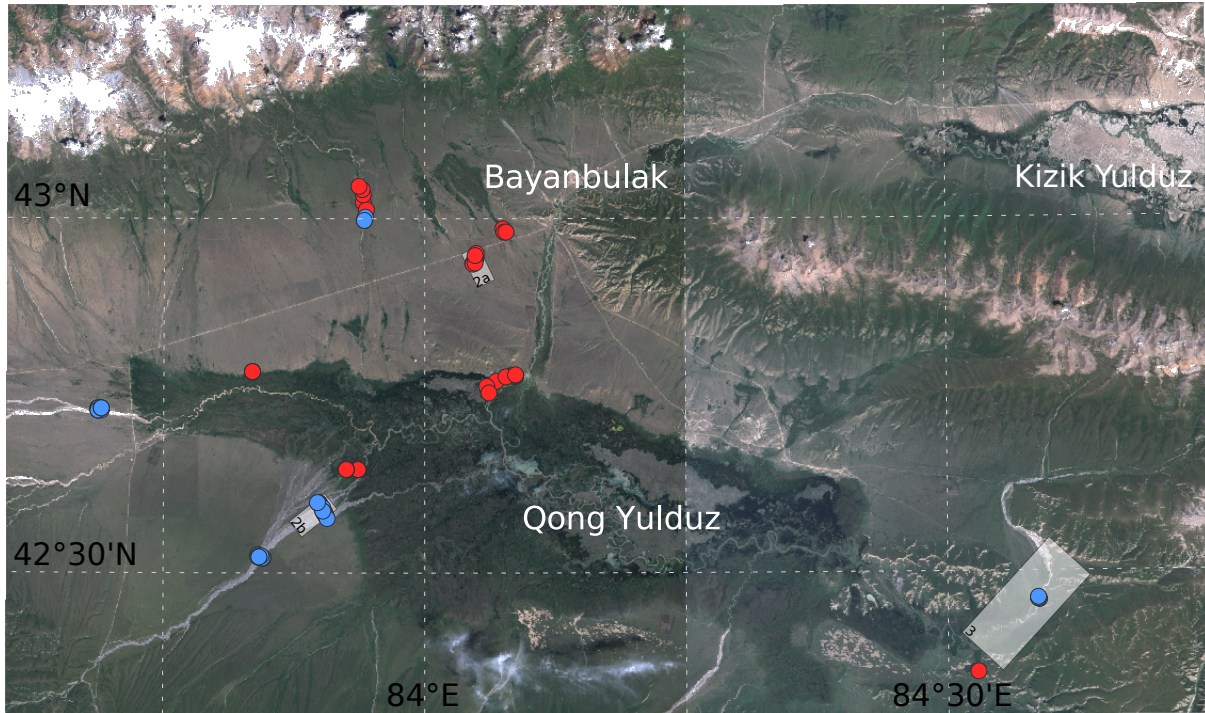


**Figure 2.** Landsat 5 mosaic image of the Bayanbulak Grassland. Red (meandering) and blue (braided) markers indicate measurement sites. White rectangles correspond to Figures 4 and 5.

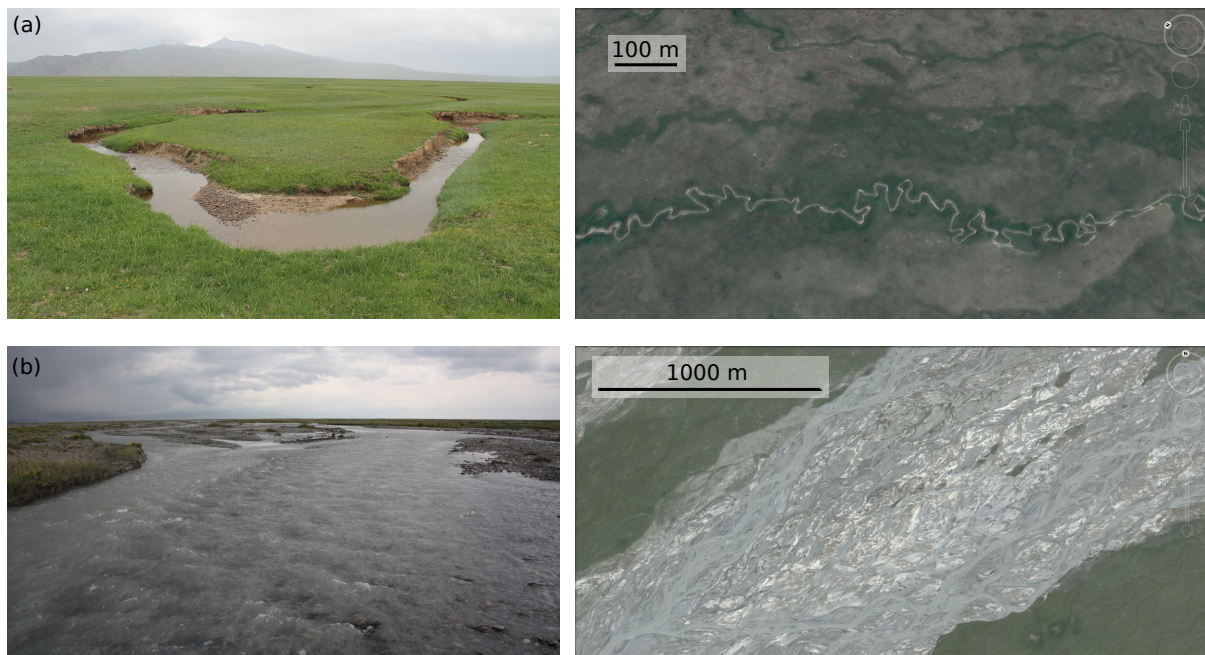


**Figure 4.** (a) Meandering and (b) braided rivers in the Bayanbulak Grassland. Left: field picture; right: satellite image (Google Earth). The corresponding locations also appear in Figure 2



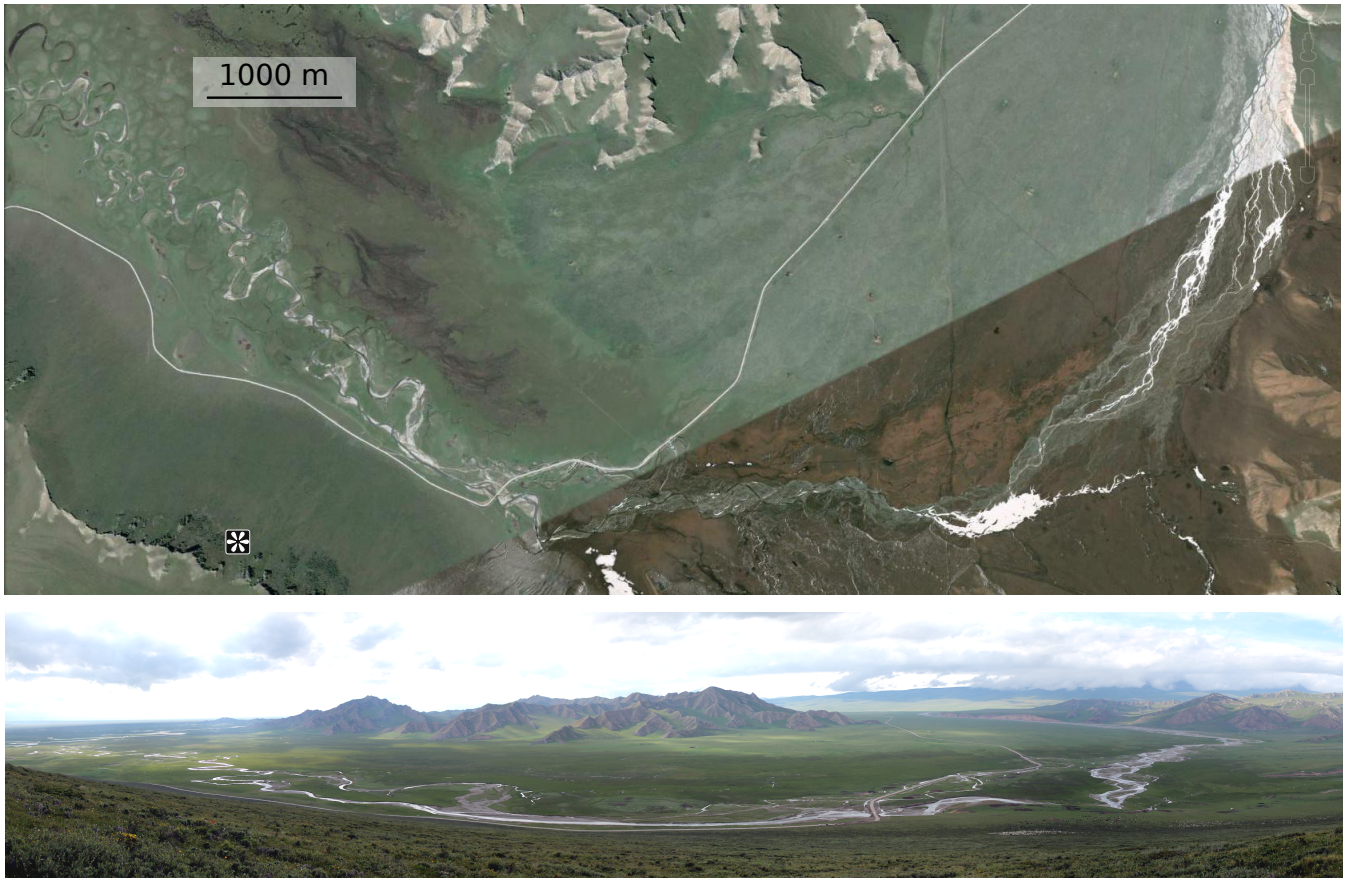


**Figure 5.** Satellite and panoramic view of a metamorphosis from braided to meandering (Bayanbulak Grassland, 84.578°E, 42.721°N, Google Earth). Marker on the satellite image indicates the viewpoint of the panoramic image. Its location also appears in Figure 2.

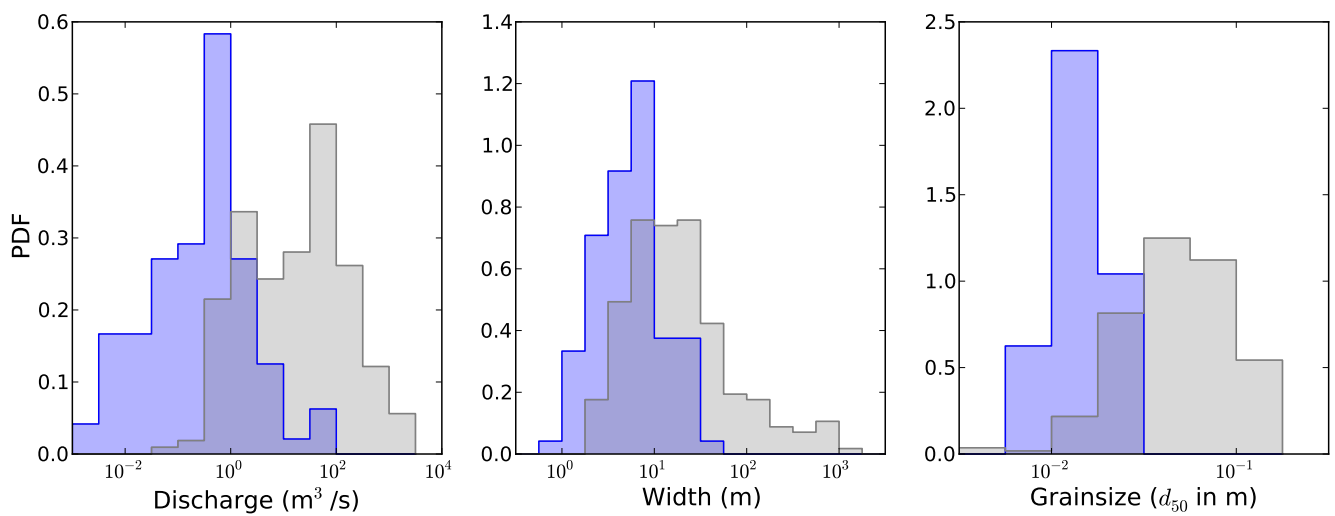


**Figure 6.** Normalized histograms (probability density function) of water discharge, width and grain size. Blue: this study; gray: GBR dataset (Church and Rood, 1983; Parker et al., 2007; King et al., 2004; Ashmore, 2013).



area at the time of measurement (Figure 1). We measured the cross-section geometry, the discharge, the grain-size distribution and the slope of the threads from as many rivers, spanning as broad a range in discharge, as possible. We chose the sections at random, according to their accessibility, our purpose being to collect a statistically significant dataset.

To measure the cross section and the water discharge of large rivers, we used a 2Mhz acoustic Doppler current profiler (ADCP, Teledyne-RDI StreamPro). The instrument was mounted on a raft and cross-sections were performed from which we extracted both the geometry and the discharge of the threads.

In shallower rivers, we used wading rods and rulers to measure the thread geometry. The mean surface velocity was measured using floats. The average velocity was obtained from the surface velocity using a correction factor of 0.6 (Sanders, 1998; Gaurav et al., 2015). The discharge was obtained by the product of the average velocity with the wetted area.

Repeated ADCP profiles across the same section show that discharge, width and depth measurements are all reproducible within less than 15 %. Manual measurements yield an uncertainty of about 2 % for width, 12 % for depth and 25 % for velocity. The resulting uncertainty on discharge is less than 40 % for both methods.

We used a Topcon theodolite with a laser rangefinder to measure the long profile of the threads, and estimate their slope. The length of topographic profiles varies from 100 m for small braided threads to more than 3 km for one meandering thread. Uncertainties on the location of the theodolite and atmospheric inhomogeneities curtail the precision of long-distance profiles. For our measurements, we expect the uncertainty on angles to reach 90". The corresponding absolute uncertainty on the slope of a river is about  $5 \cdot 10^{-4}$ .

We measured the grain-size distribution from surface counts. Depending on the size of exposed surfaces, the number of counts ranged from 200 to 500 (Wolman, 1954; Bunte and Abt, 2001). We extracted the median grain size  $d_{50}$  and the size of the 90<sup>th</sup> percentile  $d_{90}$  from these distributions.

Finally, the sinuosity of the threads was measured using the topographic profiles when available. When these were not available, we used Google images and calculated the sinuosity from 1 km-long stretches centered on the measurement site. The Bayanbulak rivers we surveyed exhibit two very distinct planforms. Single-thread rivers are, on average, highly meandering with a sinuosity of  $1.5 \pm 0.2$  (Schumm, 2005). The braided rivers we surveyed have a total braiding index ranging from 3.3 to almost 11.2. As our objective is to compare these two end-members, we ignored rivers with intermediate wandering morphology (Church, 1983). Overall, our dataset is composed of 92 measurements of width, depth, average velocity, discharge, slope and grain size, among which 53 correspond to braided-river threads (Table 1), and 39 to meandering-river threads (Table 2).

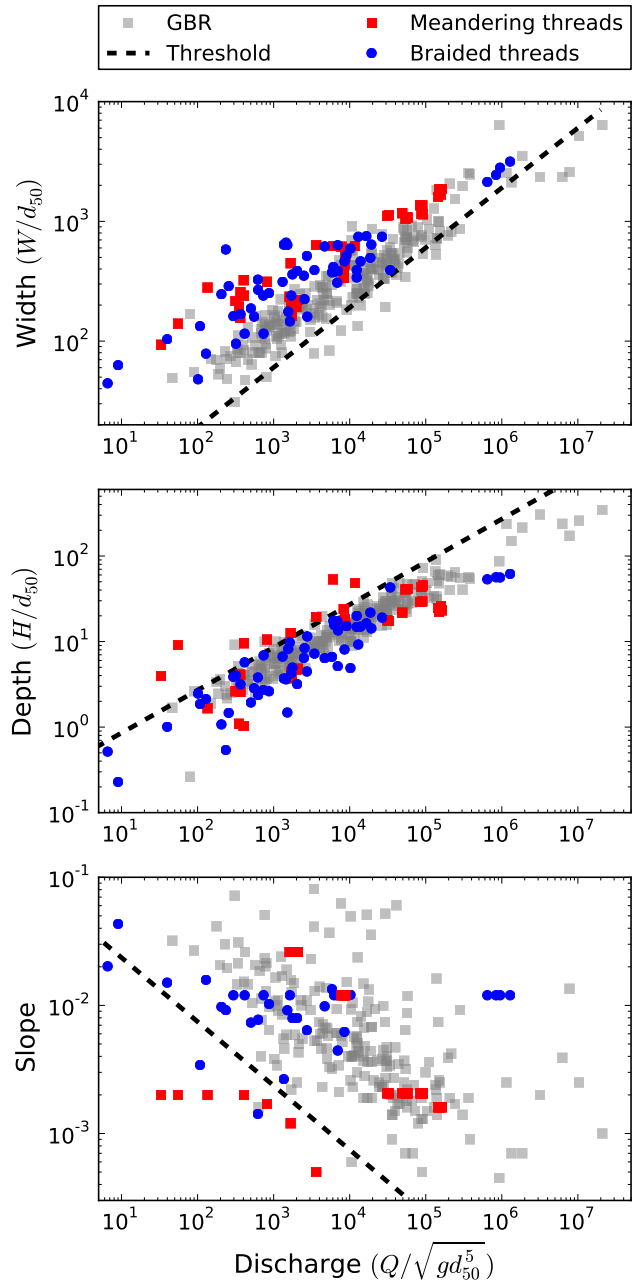


**Figure 7.** Dimensionless width, depth and slope of individual gravel-bed threads as a function of dimensionless water discharge. Dashed lines represent the threshold theory.

#### 4 Regime equations

Figure 6 compares our measurements to four other sources. Three of them, the compendiums of Parker et al. (2007), Church and Rood (1983) and King et al. (2004) include measurements from single-thread rivers. The fourth one corresponds to measurements on individual threads of the braided

Code	Lat	Lon	Channel	Measurement	$Q$	Sec	$V$	$W$	$H$	$d_{50}$	$d_{90}$	$S$
174	42.7611	83.841	B	Fl	2.9	2.6	1.1	18.0	0.14	0.028	0.064	0.0044
180	42.7617	83.8428	B	Fl	4.2	2.3	1.8	17.0	0.14	0.028	0.064	0.012
181	42.7602	83.8454	B	Fl	1.1	1.8	0.62	14.0	0.13	0.028	0.064	0.0064
182	42.7604	83.8448	B	Fl	0.36	0.52	0.69	7.0	0.073	0.028	0.064	0.01
183	42.7617	83.8439	B	Fl	0.73	1.4	0.52	10.0	0.14	0.028	0.064	0.0079
184	42.7609	83.8417	B	Fl	0.62	0.74	0.84	18.0	0.041	0.028	0.064	0.0092
185	42.7608	83.8415	B	Fl	2.4	1.9	1.2	11.0	0.19	0.028	0.064	0.013
168	42.7307	84.5878	B	Fl	0.0034	0.011	0.32	1.7	0.0062	0.027	0.064	0.043
142	42.9985	83.943	B	Fl	0.025	0.11	0.23	1.5	0.074	0.013	0.064	0.012
141	43.0004	83.9435	B	Fl	0.38	1.0	0.38	4.9	0.2	0.013	0.064	0.012
139	42.9985	83.943	B	Fl	0.41	0.9	0.46	4.0	0.23	0.013	0.064	0.012
137	43.0004	83.9435	B	Fl	0.099	0.24	0.41	1.9	0.13	0.013	0.064	0.012
179	42.7618	83.8416	B	Fl	0.84	0.96	0.87	11.0	0.089	0.028	0.064	0.008
178	42.7609	83.8413	B	Fl	0.097	0.25	0.39	16.0	0.015	0.028	0.064	0.0092
173	42.7622	83.8404	B	Fl	0.56	1.9	0.3	18.0	0.1	0.028	0.064	0.0027
172	42.7605	83.8447	B	Fl	0.21	0.28	0.72	5.3	0.054	0.028	0.064	0.0073
171	42.7608	83.8446	B	Fl	0.26	0.5	0.52	7.5	0.066	0.028	0.064	0.0077
170	42.7619	83.8416	B	Fl	1.9	3.1	0.62	17.0	0.18	0.028	0.064	0.0098
169	42.7316	84.5874	B	Fl	0.23	0.9	0.26	8.8	0.1	0.027	0.064	0.0014
175	42.7604	83.8452	B	Fl	0.084	0.21	0.41	6.9	0.03	0.028	0.064	0.0097
167	42.7314	84.5877	B	Fl	0.0025	0.017	0.15	1.2	0.014	0.027	0.064	0.02
166	42.731	84.5877	B	Fl	0.015	0.076	0.2	2.8	0.027	0.027	0.064	0.015
165	42.7305	84.5887	B	Fl	0.04	0.18	0.22	3.6	0.05	0.027	0.064	0.0034
176	42.7609	83.8419	B	Fl	3.5	2.9	1.2	13.0	0.23	0.028	0.064	0.0062
177	42.7623	83.8404	B	Fl	0.053	0.13	0.4	2.2	0.06	0.028	0.064	0.016
135	43.0004	83.9435	B	Fl	0.018	0.11	0.17	2.1	0.05	0.013	0.064	0.012
134	42.9985	83.943	B	Fl	0.044	0.13	0.33	1.5	0.09	0.013	0.064	0.012
125	42.7995	83.8983	B	Fl	0.19	0.44	0.43	4.9	0.09	0.013	0.053	0.008
111	42.7898	83.9064	B	Fl	0.03	0.071	0.43	2.0	0.036	0.013	0.053	0.008
112	42.7944	83.9025	B	Fl	1.9	2.6	0.71	4.9	0.54	0.013	0.053	0.008
113	42.7946	83.9025	B	Fl	0.14	0.29	0.47	2.8	0.1	0.013	0.053	0.008
114	42.7985	83.8993	B	Fl	1.0	1.7	0.61	6.2	0.27	0.013	0.053	0.008
115	42.799	83.8992	B	Fl	0.15	0.29	0.53	2.0	0.14	0.013	0.053	0.008
116	42.7924	83.904	B	Fl	0.0056	0.018	0.3	0.6	0.031	0.013	0.053	0.008
117	42.7911	83.9053	B	Fl	0.02	0.083	0.24	2.1	0.04	0.013	0.053	0.008
118	42.7991	83.8989	B	Fl	0.39	0.81	0.48	4.8	0.17	0.013	0.053	0.008
110	42.7983	83.8995	B	Fl	0.68	0.91	0.74	4.9	0.19	0.013	0.053	0.008
109	42.7914	83.905	B	Fl	0.14	0.35	0.39	4.4	0.08	0.013	0.053	0.008
101	42.7915	83.905	B	Fl	0.71	1.1	0.66	9.3	0.12	0.013	0.053	0.008
102	42.7921	83.9042	B	Fl	0.91	1.9	0.47	9.4	0.2	0.013	0.053	0.008
103	42.7944	83.9025	B	Fl	0.04	0.1	0.39	3.0	0.034	0.013	0.053	0.008
104	42.7946	83.9025	B	Fl	0.093	0.16	0.59	3.0	0.053	0.013	0.053	0.008
105	42.7916	83.9047	B	Fl	0.014	0.066	0.21	3.6	0.018	0.013	0.053	0.008
106	42.7985	83.8994	B	Fl	0.08	0.38	0.21	8.3	0.045	0.013	0.053	0.008
107	42.7983	83.8994	B	Fl	0.76	1.1	0.7	5.8	0.19	0.013	0.053	0.008
108	42.7898	83.9063	B	Fl	1.1	1.4	0.74	8.0	0.18	0.013	0.053	0.008
119	42.7925	83.9037	B	Fl	0.017	0.06	0.29	1.2	0.05	0.013	0.053	0.008
100	42.7925	83.9037	B	Fl	0.085	0.23	0.38	2.2	0.1	0.013	0.053	0.008
124	42.7934	83.903	B	Fl	0.5	1.2	0.4	6.5	0.19	0.013	0.053	0.008
123	42.7884	83.907	B	Fl	0.072	0.33	0.22	3.9	0.083	0.013	0.053	0.008
122	42.7926	83.9037	B	Fl	0.68	1.1	0.64	4.3	0.25	0.013	0.053	0.008
121	42.7937	83.9028	B	Fl	1.5	2.2	0.66	9.3	0.24	0.013	0.053	0.008
120	42.7953	83.9025	B	Fl	0.33	1.1	0.29	5.2	0.22	0.013	0.053	0.008
646	42.6926	83.6944	B	ADCP	51.0	24.0	2.2	35.0	0.68	0.011	0.15	0.012
649	42.6926	83.6944	B	ADCP	33.0	17.0	2.0	27.0	0.62	0.011	0.15	0.012
652	42.6926	83.6944	B	ADCP	26.0	14.0	1.9	23.0	0.59	0.011	0.15	0.012
655	42.6926	83.6944	B	ADCP	38.0	19.0	2.0	31.0	0.62	0.011	0.15	0.012

**Table 1.** Data gathered for braided-river threads. Latitude (lat) and longitude (lon) are in degrees centesimal; Measurement stands for measurement type (Fl:float, ADCP: Acoustic doppler curent profiler);  $Q$ : Discharge, Sec: wetted area,  $V$ : average velocity,  $W$ : width,  $H$ : Depth,  $d_{50}$ : median grain size,  $d_{90}$ : size of the 90<sup>th</sup> percentile,  $S$ : slope. All physical quantities are given in the International System of Units.



Code	Lat	Lon	Channel	Measurement	$Q$	Sec	$V$	$W$	$H$	$d_{50}$	$d_{90}$	$S$
614	42.8229	83.9253	M	ADCP	0.69	2.1	0.33	7.3	0.28	0.007	0.038	0.0021
626	42.8915	83.835	M	ADCP	8.2	6.5	1.3	23.0	0.28	0.013	0.03	0.0016
609	42.8227	83.9366	M	ADCP	1.1	1.9	0.56	9.5	0.2	0.007	0.038	0.0021
625	42.8915	83.835	M	ADCP	8.9	6.7	1.3	23.0	0.29	0.013	0.03	0.0016
610	42.8227	83.9366	M	ADCP	1.2	2.0	0.59	9.5	0.21	0.007	0.038	0.0021
624	42.8915	83.835	M	ADCP	7.9	6.2	1.3	20.0	0.31	0.013	0.03	0.0016
611	42.8227	83.9366	M	ADCP	1.1	2.4	0.46	8.1	0.3	0.007	0.038	0.0021
612	42.8227	83.9366	M	ADCP	1.2	2.5	0.46	8.0	0.32	0.007	0.038	0.0021
623	42.8915	83.835	M	ADCP	8.7	6.8	1.3	21.0	0.33	0.013	0.03	0.0016
613	42.8229	83.9253	M	ADCP	0.74	2.2	0.34	7.5	0.29	0.007	0.038	0.0021
617	42.8229	83.9253	M	ADCP	0.42	0.97	0.43	7.9	0.12	0.007	0.038	0.0021
616	42.8229	83.9253	M	ADCP	0.4	0.96	0.42	7.8	0.12	0.007	0.038	0.0021
615	42.8229	83.9253	M	ADCP	0.73	2.2	0.33	7.6	0.29	0.007	0.038	0.0021
608	42.8227	83.9366	M	ADCP	0.63	1.2	0.51	8.2	0.15	0.007	0.038	0.0021
144	43.0224	83.9376	M	FI	0.53	1.3	0.4	6.6	0.2	0.013	0.064	0.012
151	42.9721	84.0495	M	FI	0.0076	0.046	0.16	1.9	0.024	0.009	0.034	0.01
150	42.9901	84.0785	M	FI	0.3	0.32	0.94	3.6	0.088	0.02	0.014	0.026
149	42.9902	84.0764	M	FI	0.3	0.34	0.88	3.9	0.088	0.02	0.014	0.026
148	42.9925	84.0758	M	FI	0.37	0.42	0.87	4.4	0.096	0.02	0.014	0.026
147	42.9909	84.0781	M	FI	0.29	0.35	0.82	4.7	0.074	0.02	0.014	0.026
146	42.9679	84.0473	M	FI	0.18	0.16	1.1	2.6	0.061	0.016	0.04	0.012
145	42.9682	84.0468	M	FI	0.2	0.23	0.87	3.1	0.075	0.016	0.04	0.012
143	43.0206	83.9402	M	FI	0.5	1.1	0.45	4.9	0.23	0.013	0.064	0.012
140	43.0167	83.9418	M	FI	0.5	1.4	0.37	4.4	0.31	0.013	0.064	0.012
138	43.0059	83.945	M	FI	0.47	1.6	0.29	8.0	0.21	0.013	0.064	0.012
136	43.011	83.9416	M	FI	0.52	1.4	0.39	5.7	0.24	0.013	0.064	0.012
152	42.9713	84.049	M	FI	0.0088	0.053	0.17	2.3	0.023	0.009	0.034	0.01
153	42.9751	84.0496	M	FI	0.0088	0.052	0.17	1.4	0.037	0.009	0.034	0.01
164	42.8769	84.0626	M	FI	0.52	7.4	0.07	9.3	0.8	0.015	0.034	0.00015
163	42.8895	84.0873	M	FI	0.012	0.1	0.11	4.2	0.025	0.015	0.034	0.002
162	42.8881	84.0782	M	FI	0.14	1.3	0.11	6.7	0.19	0.015	0.034	0.0012
161	42.8812	84.0603	M	FI	1.0	6.7	0.15	9.3	0.72	0.015	0.034	0.00015
160	42.8887	84.0836	M	FI	0.071	0.74	0.095	4.7	0.16	0.015	0.034	0.0017
159	42.889	84.0881	M	FI	0.0029	0.083	0.035	1.4	0.059	0.015	0.034	0.002
158	42.8852	84.0688	M	FI	0.31	2.8	0.11	9.5	0.29	0.015	0.034	0.0005
157	42.889	84.0861	M	FI	0.035	0.52	0.068	3.6	0.14	0.015	0.034	0.002
156	42.8891	84.088	M	FI	0.0048	0.29	0.017	2.1	0.14	0.015	0.034	0.002
155	42.9733	84.0494	M	FI	0.0084	0.017	0.49	1.8	0.0099	0.009	0.034	0.01
154	42.9686	84.0489	M	FI	0.0097	0.027	0.36	2.9	0.0093	0.009	0.034	0.01

**Table 2.** Data gathered for meandering-river threads. Latitude (lat) and longitude (lon) are in degrees centesimal; Measurement stands for measurement type (FI:float, ADCP: Acoustic doppler curren profiler);  $Q$ : Discharge, Sec: wetted area,  $V$ : average velocity,  $W$ : width,  $H$ : Depth,  $d_{50}$ : median grain size,  $d_{90}$ : size of the 90<sup>th</sup> percentile,  $S$ : slope. All physical quantities are given in the International System of Units.

Sunwapta River (Ashmore, 2013). These sources are hereafter referred to as the GBR dataset.

The Bayanbulak threads are widely dispersed in size ( $0.6 \leq W \leq 35$  m), and discharge ( $0.002 \leq Q \leq 51$  m<sup>3</sup>s<sup>-1</sup>). On average, they are smaller than the GBR threads. The median grain size of the Bayanbulak threads  $d_{50} \approx 0.013$  m is finer (the standard deviation of the  $d_{50}$  is  $\sigma_{d_{50}} \sim 0.008$  m). Our dataset therefore extend the GBR ones towards smaller threads with finer sediments.

We now consider the empirical regime equations of individual threads (Figure 7). To facilitate the comparison between the GBR dataset and our own, we use dimensionless quantities, namely  $W/d_{50}$ ,  $H/d_{50}$ ,  $S$  and  $Q_* = Q/\sqrt{gd_{50}^3}$ , where  $g$  is the acceleration of gravity. Not surprisingly, the geometry of a thread is strongly correlated with its water discharge: its width and depth increase with discharge, while its slope decreases. At first sight, these trends are similar for meandering and braided threads. They also compare well to the GBR data set, although the Bayanbulak threads are slightly wider than the GBR ones on average. The measurement uncertainty, although significant, is less than the variability of our data, except for slopes smaller than about  $5 \cdot 10^{-3}$ .

Despite considerable scatter, both our measurements and the GBR datasets gather around straight lines in the log-log plots of Figure 7, suggesting power-law regime equations:

$$\frac{W}{d_{50}} = \alpha_w Q_*^{\beta_w}; \quad \frac{H}{d_{50}} = \alpha_h Q_*^{\beta_h}; \quad S = \alpha_s Q_*^{\beta_s} \quad (1)$$

where  $\alpha_w$ ,  $\alpha_h$ ,  $\alpha_s$ ,  $\beta_w$ ,  $\beta_h$  and  $\beta_s$  are dimensionless parameters. To evaluate them, we use reduced major axis regression (RMA) instead of least square regression because the variability of our data is comparable along both axes (Sokal and Rohlf, 1995; Scherrer, 1984). The resulting fitted coefficients are reported in Table 3. The scatter in the slope measurement is too large to provide significant estimates of the slope coefficients  $\alpha_s$  and  $\beta_s$ . At the 95% confidence level, the regime relationships of meandering and braided threads cannot be distinguished. Similarly, the depth of the Bayanbulak threads cannot be distinguished from those of the GBR threads. Conversely, the Bayanbulak threads are significantly wider than the GBR threads with respect to their median grain size.

So far we have made the width, depth and discharge dimensionless using  $d_{50}$  as the characteristic grain size of the sediment. This choice, however, is arbitrary (Parker et al., 2007; Parker, 2008). Large grains are arguably more likely to control the geometry of the threads than smaller ones, and a larger quantile might be a better approximation of the characteristic grain size. For comparison, we rescaled our measurements using  $d_{90}$  instead of  $d_{50}$ , and repeated the above analysis. Our conclusions are not altered significantly by this choice of characteristic grain size (Table 3).

Width: $\log_{10}(W/d_s) = \beta_w \log_{10} Q_* + \alpha_w$					
Thread	$d_s$	$\beta_w$	$\alpha_w$	$\sigma_{\beta_w}$	$R^2$
Total Pop.	$d_{50}$	0.33	1.47	0.03	0.83
	$d_{90}$	0.34	1.35	0.04	0.78
Meandering	$d_{50}$	0.35	1.38	0.04	0.91
	$d_{90}$	0.33	1.37	0.04	0.91
Braided	$d_{50}$	0.32	1.51	0.05	0.78
	$d_{90}$	0.35	1.34	0.07	0.66
GBR	$d_{50}$	0.41	0.86	0.02	0.87
	$d_{90}$	0.49	0.78	0.04	0.94
Depth: $\log_{10}(H/d_s) = \beta_h \log_{10} Q_* + \alpha_h$					
Thread type	$d_s$	$\beta_h$	$\alpha_h$	$\sigma_{\beta_h}$	$R^2$
Total Pop.	$d_{50}$	0.44	-0.62	0.04	0.84
	$d_{90}$	0.4	-0.5	0.05	0.77
Meandering	$d_{50}$	0.44	-0.66	0.08	0.84
	$d_{90}$	0.39	-0.46	0.08	0.8
Braided	$d_{50}$	0.44	-0.61	0.05	0.83
	$d_{90}$	0.41	-0.51	0.07	0.7
GBR	$d_{50}$	0.45	-0.63	0.02	0.92
	$d_{90}$	0.34	-0.29	0.04	0.9

**Table 3.** Linear regressions on the  $\log_{10}$  of width and depth as functions of discharge and for two characteristic grain sizes. The confidence level is 95%. RMA: Reduced major axis regression  $\sigma_{\beta}$  stands for confidence interval on the slope of the regression  $\beta$ .

## 5 Detrending

So far, we have found that the empirical regime equations of meandering and braided threads are statistically similar. To proceed further with this comparison, we would like to convert our measurements into a single statistical ensemble. We thus need to detrend our dataset with respect to water discharge, based on analytical regime equations. Following Gaurav et al. (2015), we propose to use the threshold theory to do so.

The threshold theory assumes that a river transports its sediment load slowly enough for its bed to be near the threshold of motion (Glover and Florey, 1951; Henderson, 1963; Yalin and Ferreira da Silva, 2001; Seizilles, 2013). Momentum and mass balances then yield power-law regime equations, the original formulation of which reads (Glover and Florey, 1951)

$$\frac{W}{d_s} = \left[ \frac{\pi}{\sqrt{\mu}} \left( \frac{\theta_t(\rho_s - \rho)}{\rho} \right)^{-1/4} \sqrt{\frac{3C_f}{2^{3/2}\mathcal{K}[1/2]}} \right] Q_*^{1/2}, \quad (2)$$

$$\frac{H}{d_s} = \left[ \frac{\sqrt{\mu}}{\pi} \left( \frac{\theta_t(\rho_s - \rho)}{\rho} \right)^{-1/4} \sqrt{\frac{3\sqrt{2}C_f}{\mathcal{K}[1/2]}} \right] Q_*^{1/2}, \quad (3)$$

$$S = \left[ \left( \mu^{1/2} \frac{\theta_t(\rho_s - \rho)}{\rho} \right)^{5/4} \sqrt{\frac{\mathcal{K}[1/2]2^{3/2}}{3C_f}} \right] Q_*^{-1/2}, \quad (4)$$



where

$$Q_* = \frac{Q}{\sqrt{gd_s^3}}, \quad (5)$$

is the dimensionless discharge.  $\rho = 1000 \text{ kg/m}^3$  and  $\rho_s = 2650 \text{ kg/m}^3$  are the densities of water and sediment,  $C_f \approx 0.1$  is the turbulent friction coefficient,  $Q$  the water discharge,  $\theta_t \sim 0.04$  the threshold Shields parameter,  $\mu \sim 0.7$  the friction angle for gravel, and  $\mathcal{K}[1/2] \approx 1.85$  a transcendental integral (Glover and Florey, 1951; Henderson, 1963; Seizilles et al., 2013).

This formulation is similar to the one proposed by Parker et al. (2007), but for two points. First, equations (2) to (4) represent a threshold channel, whereas Parker et al. (2007) extend the theory to active channels. Second, the formulation of Glover and Florey (1951) uses a constant friction coefficient in the momentum balance, whereas Parker et al. (2007) use a more elaborate friction law. Here we use the simplest formulation, as the variability of our data overshadows these differences (Metivier and Barrier, 2012).

The dashed lines on Figure 7 represent equations (2) to (4). On average, the Bayanbulak threads are wider, shallower and steeper than the corresponding threshold thread. However, the theory predicts reasonably their dependence with respect to discharge, thus supporting its use to detrend our data. Accordingly, we define a set of rescaled quantities as follows:

$$W_* = \frac{W}{d_s C_W \sqrt{Q_*}} = \frac{W(gd_s)^{1/4}}{C_W \sqrt{Q}}, \quad (6)$$

$$H_* = \frac{H}{d_s C_H \sqrt{Q_*}} = \frac{H(gd_s)^{1/4}}{C_H \sqrt{Q}}, \quad (7)$$

$$S_* = S \frac{\sqrt{Q_*}}{C_S} = \frac{S \sqrt{Q}}{g^{1/4} d_s^{5/4} C_S}. \quad (8)$$

Here the coefficients  $C_W, C_H, C_S$  correspond to the prefactors in square brackets of equations (2) to (4). We used the typical values reported above for the coefficients that do not vary in our dataset.

Figure 8 shows the relationship between the rescaled thread geometry and its dimensionless discharge, using  $d_{50}$  to approximate the characteristic grain size  $d_s$ . The new quantities  $W_*, H_*$  and  $S_*$  appear far less dependent on the water discharge than their original counterpart, although a residual trend remains for all of them. Using ordinary least squares, we fit power laws to our rescaled data to evaluate this residual trend. We find  $W_* \propto Q_*^{-0.19 \pm 0.03}$  and  $H_* \propto Q_*^{-0.10 \pm 0.05}$  for the Bayanbulak threads, and  $W_* \propto Q_*^{-0.1 \pm 0.02}$  and  $H_* \propto Q_*^{-0.05 \pm 0.02}$  for the GBR threads. The width of the Bayanbulak threads shows the strongest correlation, yet even this correlation is mild. Finally, slopes are more strongly correlated with discharge than width and depth both for the GBR threads ( $S_* \propto Q_*^{0.21 \pm 0.05}$ ), and the Bayanbulak threads ( $S_* \propto Q_*^{0.39 \pm 0.11}$ ). However, most of the difference between

Width $\log_{10}(W_*)$			
River type	Grain size	Mean	Standard deviation
Meandering	$d_{50}$	0.6	0.3
Meandering	$d_{90}$	0.8	0.2
Braided	$d_{50}$	0.7	0.3
Braided	$d_{90}$	0.8	0.2
GBR	$d_{50}$	0.3	0.2
GBR	$d_{90}$	0.5	0.1
Depth $\log_{10}(H_*)$			
River type	Grain size	Mean	Standard deviation
Meandering	$d_{50}$	-0.1	0.3
Meandering	$d_{90}$	-0.0	0.3
Braided	$d_{50}$	-0.2	0.2
Braided	$d_{90}$	-0.1	0.2
GBR	$d_{50}$	-0.2	0.1
GBR	$d_{90}$	-0.0	0.2
Slope $\log_{10}(S_*)$			
River type	Grain size	Mean	Standard deviation
Meandering	$d_{50}$	0.4	0.7
Meandering	$d_{90}$	-0.22	0.74
Braided	$d_{50}$	0.5	0.7
Braided	$d_{90}$	-0.11	0.46
GBR	$d_{50}$	0.7	0.4
GBR	$d_{90}$	-0.05	0.24
Aspect Ratio $\log_{10}(W/H)$			
River type	Grain size	Mean	Standard deviation
Meandering	-	0.8	0.3
Braided	-	0.9	0.4
GBD	$d_{50}$	0.5	0.2

**Table 4.** Mean and standard deviations of the logarithms of detrended widths, depths and slopes. The aspect ratios is naturally detrended and does not depend on grain size.

the Bayanbulak and GBR threads is due to slopes well below the measurement precision. In all cases, the scatter is large, and all correlations fall within the standard deviation of the dataset.

## 6 Thread geometry

We now analyze our rescaled measurements as a homogeneous statistical ensemble (Figure 8). The means of the rescaled distributions of width, depth and slope all fall about one order of magnitude away from one, and their dispersion around this mean is also about one order of magnitude (table 4). This observation supports the use of the threshold theory to scale the morphology of the Bayanbulak rivers.

The dispersion of the rescaled slope is more significant than that of width and depth. We believe that, in addition to the technical difficulties associated to the measurement of slope in the field (section 3), the dispersion of the grain size explains this scatter. Indeed, gravels are broadly distributed in size, and unevenly distributed over the river bed (Guerit et al., 2014). Since the rescaling for slope involves the grain

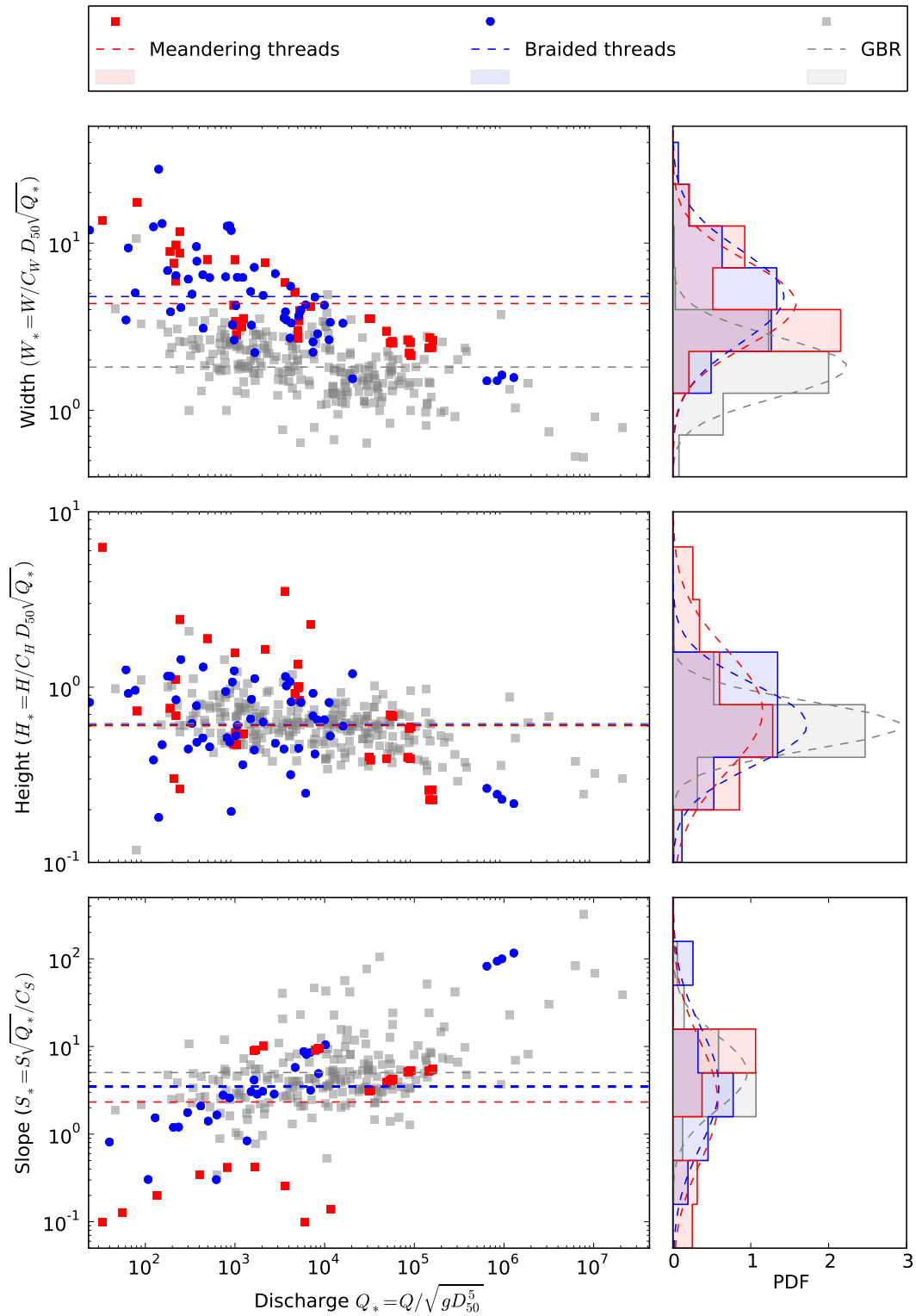


**Figure 8.** Left: rescaled width ( $W_*$ ), depth ( $H_*$ ) and slope ( $S_*$ ) as a function of rescaled water discharge ( $Q_*$ ). Rescaled quantities are from equations (6) to (8). Threshold rivers correspond to rescaled width, depth and slope equal to 1. Right: probability density function of rescaled quantities, with fitted lognormal distributions.



size  $d_s$  to the power of  $5/4$ , whereas this exponent is only  $1/4$  for width and depth (equations (6) to (8)), we believe the grain-size dispersion impacts more strongly the rescaled slope than the rescaled width and depth.

The means of the distributions for braided threads and meandering threads differ by less than a factor of two, much smaller than the standard deviation. Fitting lognormal distributions to our data, we find that the meandering and braided threads from Bayanbulak cannot be distinguished from each other, at the 95% level of confidence. The depth and slope of the Bayanbulak threads are also not significantly different from the GBR threads. Finally, the width of the Bayanbulak threads is larger than that of the GBR ones. We therefore conclude that, within the natural variability of our observation, the sections of meandering and braided threads are geometrically similar although the morphology of the braided and meandering rivers looks qualitatively different (Figures 2 and 4). Again, the use of  $d_{90}$  instead of  $d_{50}$  as a characteristic grain size does not alter this conclusion.

According to the rescaling equations (6) to (8) the aspect ratio of a river  $W/H$  should be naturally detrended (Figure 9). Indeed, the correlation coefficient of aspect ratio and discharge is less than 0.01 for all datasets. As expected, the aspect ratio of braided and meandering threads cannot be distinguished at the 95% level of confidence. Finally, the difference between the width of the Bayanbulak threads and that of the GBR threads also appears in the distribution of aspect ratios: the Bayanbulak aspect ratios are larger than the GBR ones.

## 7 Conclusion

Our measurements on gravel-bed rivers in the Bayanbulak Grassland reveal that braided threads are geometrically similar to meandering ones. Their size can be virtually detrended with respect to water discharge using the threshold theory. As a result, their aspect ratio is naturally detrended. These findings accord with recent observations in sand-bed rivers of the Kosi Megafan (Gaurav et al., 2015). They also accord with recent results from rivers of the Ganges-Brahmaputra plain (Gaurav, 2016).

The striking similarity between braided and meandering threads in gravel-bed and sand-bed rivers supports the view that fully-developed braided rivers are essentially a collection of threads interacting with each other, rather than a single wide channel segmented by sediment bars. If confirmed, this would suggest that a braid results from the collective behavior of individual threads, the property and dynamics of which would be close to that of meandering threads (Sinha and Friend, 1994; Ashmore, 2013; Reitz et al., 2014).

Our observations, like those of Gaurav et al. (2015) or the GBR dataset, are much dispersed around their average value, which points at the influence of hidden parameters on their morphology. Among those, the intensity of sediment trans-

port is likely to play a prominent role, at least in the case of the Bayanbulak rivers where both vegetation and grain-size distributions are relatively uniform over the grassland.

More specifically, field observations suggest that a heavier sediment load tends to increase the aspect ratio of a thread, other things being equal (Smith and Smith, 1984; Tal and Paola, 2010; Metivier and Barrier, 2012). This proposition remains speculative though, and needs to be thoroughly tested against dedicated field measurements, which we believe should include both braided and meandering threads. Finally, if the sediment discharge is indeed the most prominent parameter after water discharge, its influence on the geometry of a channel should also manifest itself in laboratory experiments.

## References

- Andrews, E. D. (1984). Bed-material entrainment and hydraulic geometry of gravel-bed rivers in Colorado. *Geol. Soc. of Am. Bull.*, 95:371–378.
- Ashmore, P. (2013). *Fluvial Geomorphology*, volume 9 of *Treatise on Geomorphology*, chapter Morphology and dynamics of braided rivers, pages 289–312. Academic Press, San Diego, CA.
- Ashmore, P. E. (1991). How do gravel-bed rivers braid? *Canadian Journal of Earth Sciences*, 28(3):326–341.
- Brauderick, C. A., Dietrich, W. E., Leverich, G. T., and Sklar, L. S. (2009). Experimental evidence for the conditions necessary to sustain meandering in coarse-bedded rivers. *Proc. Nat. Acad. Sci.*
- Bunte, K. and Abt, S. (2001). Sampling surface and subsurface particle-size distributions in wadable gravel- and cobble-bed streams for analyses in sediment transport, hydraulics, and streambed monitoring. Technical report.
- Church, M. (1983). Pattern of instability in a wandering gravel bed channel. *Modern and ancient fluvial systems. International Association of Sedimentologists, Special Publication*, 6:169–180.
- Church, M. and Gilbert, R. (1975). *Glaciofluvial and glaciolacustrine sedimentation*, volume 23 of *Special Publication*, chapter Proglacial Fluvial and Lacustrine Environments, pages 22–100. SEPM.
- Church, M. and Rood, K. (1983). Catalogue of Alluvial River Channel Regime Data. *Univ. British Columbia, Department of Geography, Vancouver*.
- Devauchelle, O., Jossierand, C., Lagrée, P., and Zaleski, S. (2007). Morphodynamic modeling of erodible laminar channels. *Physical Review E*, 76(5):056318.
- Dijk, W., Lageweg, W., and Kleinhans, M. (2012). Experimental meandering river with chute cutoffs. *Journal of Geophysical Research: Earth Surface (2003–2012)*, 117(F3).
- Ferguson, R. (1987). *Hydraulic and sedimentary controls of channel pattern*. Blackwell Oxford, UK.
- Fredsøe, J. (1978). Meandering and braiding of rivers. *Journal of Fluid Mechanics*, 84(04):609–624.
- Fujita, Y. and Muramoto, Y. (1985). Studies on the process of development of alternate bars.
- Gaurav, K. (2016). *Morphology of alluvial rivers*. PhD thesis, IPGP.
- Gaurav, K., Métivier, F., Devauchelle, O., Sinha, R., Chauvet, H., Houssais, M., and Bouquerel, H. (2015). Morphology of the kosi

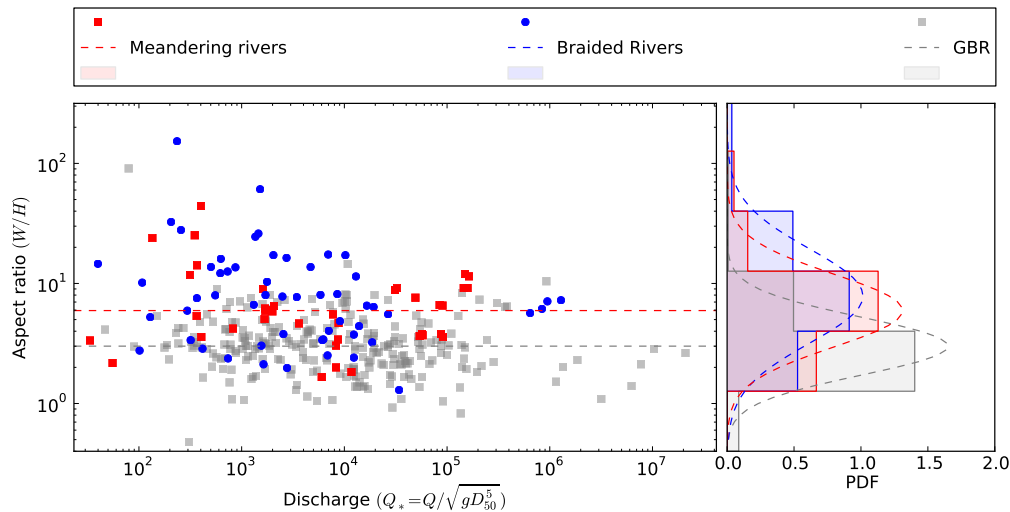


**Figure 9.** Aspect ratio of braided and meandering threads from Bayanbulak and the GBR datasets, as a function of rescaled water discharge ( $Q_*$ ).

- megafan channels. *Earth Surface Dynamics*, 3(3):321–331.
- Glover, R. E. and Florey, Q. (1951). *Stable channel profiles*. US Department of the Interior, Bureau of Reclamation, Design and Construction Division.
- Gran, K. and Paola, C. (2001). Riparian vegetation controls on braided stream dynamics. *Water Resources Research*, 37(12):3275–3283.
- Guerit, L., Barrier, L., Narteau, C., Métivier, F., Liu, Y., Lajeunesse, E., Gayer, E., Meunier, P., Malverti, L., and Ye, B. (2014). The grain-size patchiness of braided gravel-bed streams &ndash; example of the urumqi river (northeast tian shan, china). *Advances in Geosciences*, 37:27–39.
- Henderson, F. M. (1963). Stability of alluvial channels. *Transactions of the American Society of Civil Engineers*, 128(1):657–686.
- King, J. G., Emmett, W. W., Whiting, P. J., Kenworthy, R. P., and Barry, J. J. (2004). Sediment transport data and related information for selected coarse-bed streams and rivers in Idaho. Gen. Tech. Rep. RMRS-GTR-131. Fort Collins, CO RMRS-GTR-131, U.S. Department of Agriculture, Forest Service, Rocky Mountain Research Station, Fort Collins, CO.
- Kleinhans, M. G. and van den Berg, J. H. (2011). River channel and bar patterns explained and predicted by an empirical and a physics-based method. *Earth Surface Processes and Landforms*, 36(6):721–738.
- Leopold, L. B. and Wolman, M. G. (1957). River Channel Patterns. Technical Report 282-B.
- Métivier, F. and Barrier, L. (2012). Alluvial landscape evolution: what do we know about metamorphosis of gravel bed meandering and braided streams. In Church, M., Biron, P., and Roy, A., editors, *Gravel-bed Rivers: processes, tools, environments.*, chapter 34, pages 474–501. Wiley & Sons, Chichester.
- Mosley, M. (1983). Response of braided rivers to changing discharge. *Journal of hydrology. New Zealand*, 22(1):18–67.
- Parker, G. (1976). On the cause and characteristic scales of meandering and braiding in rivers. *Journal of Fluid Mechanics*, 76(3):457–480.
- Parker, G. (2008). Transport of gravel and sand mixtures. In Garcia, M. H., editor, *Sedimentation engineering: processes, management, modeling, and practice*, volume 110, chapter 3, pages 165–251. ASCE.
- Parker, G., Wilcock, P., Paola, C., Dietrich, W. E., and Pitlick, J. (2007). Quasi-universal relations for bankfull hydraulic geometry of single-thread gravel-bed rivers. *Journal of Geophysical Research–Earth Surface*, 112:1–21.
- Reitz, M. D., Jerolmack, D. J., Lajeunesse, E., Limare, A., Devauchelle, O., and Métivier, F. (2014). Diffusive evolution of experimental braided rivers. *Phys. Rev. E*, 89:052809.
- Sanders, L. (1998). A manual of field hydrogeology. *Prentice-Hall, Inc.*, 113 Sylvan Ave. Englewood Cliffs NJ 07632 USA. 381, page 1998.
- Scherrer, B. (1984). *Biostatistique*. Chicoutimi, Québec: G. Morin.
- Schumm, S. A. (2005). *River variability and complexity*. Cambridge Univ Pr.
- Seizilles, G. (2013). *Forme d’équilibre d’une rivière*. PhD thesis, Université Paris Diderot.
- Seizilles, G., Devauchelle, O., Lajeunesse, E., and Métivier, F. (2013). Width of laminar laboratory rivers. *Phys. Rev. E*, 87:052204.
- Sinha, R. and Friend, P. (1994). River systems and their sediment flux, indo-gangetic plains, northern bihar, india. *Sedimentology*, 41(4):825–845.
- Smith, N. D. and Smith, D. G. (1984). William River: An outstanding example of channel widening and braiding caused by bed-load addition. *Geology*, 12(2):78.
- Sokal, R. and Rohlf, F. (1995). *Biometry*.
- Tal, M. and Paola, C. (2007). Dynamic single-thread channels maintained by the interaction of flow and vegetation. *Geology*, 35(4):347.

- Tal, M. and Paola, C. (2010). Effects of vegetation on channel morphodynamics: results and insights from laboratory experiments. *Earth Surf. Proc. Landf.*, 35(9):1014–1028.
- Wolman, M. G. (1954). A method for sampling coarse river bed material. *EOS Trans. AGU*, 36:655–663.
- Yalin, M. S. and Ferreira da Silva, A. M. (2001). *Fluvial Processes*. International Association of Hydraulic Engineering and Research Monograph.
- Yang, Q. and Cui, C. (2005). Impact of climate change on the surface water of kaidu river basin. *Journal of Geographical Sciences*, 15(1):20–28.
- Zhang, B., Yao, Y.-h., Cheng, W.-m., Zhou, C., Lu, Z., Chen, X., Alshir, K., ErDowlet, I., Zhang, L., and Shi, Q. (2002). Human-induced changes to biodiversity and alpine pastureland in the bayanbulak region of the east tienshan mountains. *Mountain research and development*, 22(4):383–389.
- Zhang, Y., Li, B., Bao, A., Zhou, C., Chen, X., and Zhang, X. (2007). Study on snowmelt runoff simulation in the kaidu river basin. *Science in China Series D: Earth Sciences*, 50(1):26–35.
- Zolezzi, G., Bertoldi, W., and Tubino, M. (2012). Morphodynamics of bars in gravel-bed rivers: Bridging analytical models and field observations. *Gravel-Bed Rivers: Processes, Tools, Environments*, pages 69–89.

### Acknowledgments

This paper is dedicated to the dear memory of Pr. Baisheng Ye. The Bayanbulak field campaign was the last we carried out together, before he accidentally died on assignment in Tibet. This work is under the aegis of the SALADYN international associated laboratory. It is IGP contribution 3685.